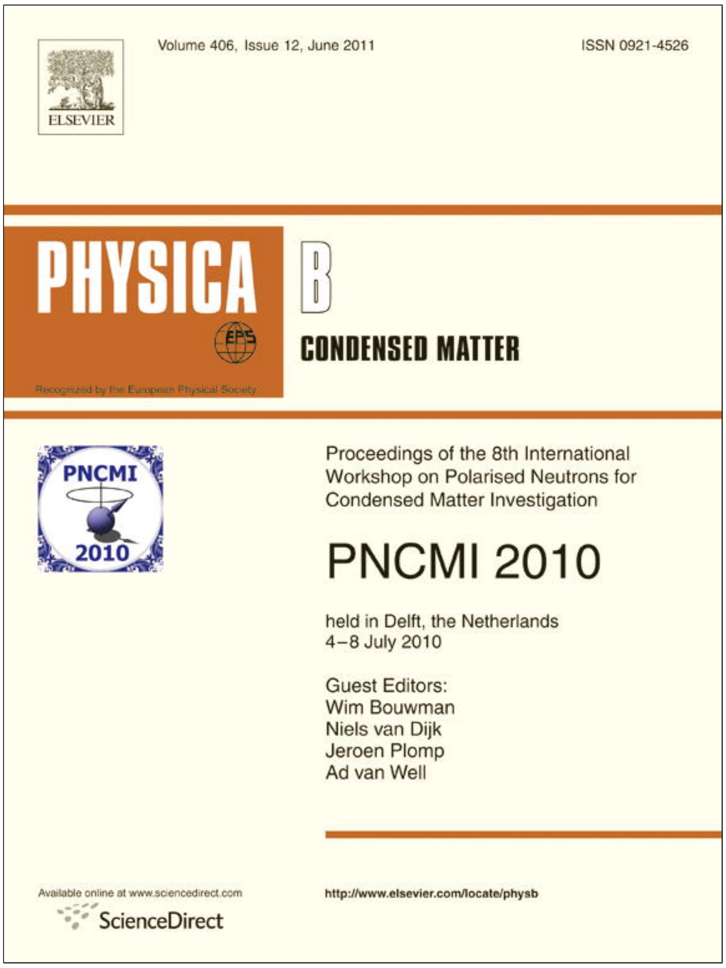

Volume 406, Issue 12, June 2011
ISSN 0921-4526

ELSEVIER

PHYSICA B
CONDENSED MATTER

Recognized by the European Physical Society

Proceedings of the 8th International
Workshop on Polarised Neutrons for
Condensed Matter Investigation

PNCMI 2010

held in Delft, the Netherlands
4–8 July 2010

Guest Editors:
Wim Bouwman
Niels van Dijk
Jeroen Plomp
Ad van Well

Available online at www.sciencedirect.com
ScienceDirect

http://www.elsevier.com/locate/physb

Physica B 406 (2011) 2405–2408

Contents lists available at ScienceDirect

Physica B

journal homepage: www.elsevier.com/locate/physb

Magnetic properties of cobalt nanowires: Study by polarized SANS

A.P. Chumakov [a,*], S.V. Grigoriev [a], N.A. Grigoryeva [b], K.S. Napolskii [c], A.A. Eliseev [c], I.V. Roslyakov [c], A.I. Okorokov [a], H. Eckerlebe [d]

[a] Petersburg Nuclear Physics Institute, Gatchina, 188300 St. Petersburg, Russia
[b] Faculty of Physics, St. Petersburg State University, 198504 St. Petersburg, Russia
[c] High School of Materials Science, Moscow State University, 119899 Moscow, Russia
[d] GKSS Forschungszentrum, 21502 Geesthacht, Germany

ARTICLE INFO

Available online 3 November 2010

Keywords:
Anodic aluminium oxide
Magnetic nanowires
Polarized small-angle neutron diffraction

ABSTRACT

Structural and magnetic properties of two-dimensional spatially ordered system of ferromagnetic cobalt nanowires embedded into Al_2O_3 matrix have been studied using polarized small-angle neutron scattering. A comprehensive analysis of contributions to the scattering intensity was carried out, including nonmagnetic (nuclear) contribution, magnetic contribution depending on the magnetic field, and nuclear–magnetic interference indicating the correlation between the magnetic and nuclear structures. Experiments have revealed an anomalously low value of the magnetic contribution as compared to the nuclear one. This behavior is interpreted in terms of low coherence of the magnetic structure caused by the anisotropy of Co crystallites as compared with the large coherency of nuclear structure of nanowires.

The investigations of the magnetic properties of ferromagnetic nanoparticles are one of the urgent problems in modern science and nanoindustry. Nanoparticles can have different shapes, such as spherical, ellipsoidal, stick-like, and others. Having a relative simplicity of their production and technological instrumental integration, cylindrical nanowires are the objects of the current researchers' attention. The main problem of these studies is the magnetic behavior of an individual magnetic particle and their array in different spatial environment and circumstances (T, P, H). For example, the evolution of the magnetization reversal mechanism of nanowires arrays with different ratios of wire's length, L, to its diameter, D, was thoroughly studied [1]. The authors carried out measurements hysteresis loop of magnetization at different orientations of the nanowires axis with respect to the magnetic field. Quantitative analysis of the M–H loops allowed them to plot the dependence of the coercitivity on the angle of mutual orientation of field and nanowire's axis. This angular dependence allows one to distinguish between two different remagnetization mechanisms, which are realised in single defect-free ellipsoids: coherent reversal mode [2] or curling reversal mode [3]. It was found that the remagnetization of nanowires with relatively large length ($L/D \geq 1$) is characterized by the curling mechanism, while upon transformation of nanowire into nanodot ($L/D < 1$) their remagnetization is characterized by the coherent mechanism. However, it must be noticed that the above-mentioned reversal mechanisms are not applicable in case when the magnetic field is applied perpendicularly to the principal wire's axis. For the long nanowires, a combination of both mechanisms (the coherent rotation and curling mode) can be suggested for the explanation [1]; however, this problem remains unsolved. The case of nanodots arrays in the perpendicular field has been recently studied in detail [4]. It was shown that the magnetic vertices appear in the range of small magnetic field with a certain chirality and polarity. Therefore, it is the curling mode that is realized in this case. In this article the remagnetization mechanism of the magnetic nanowires at perpendicular orientation of the field with respect to the wire axis is investigated by polarized SANS, and based on the obtained data we have concluded that the small magnetic coherent volume and polycrystalline nature of the nanowires play the dominating role in their reversal mechanism.

The subject of the study is the cobalt nanowires arrays embedded into anodic alumina. Chosen technique of polarized small-angle neutron scattering is sensitive to the structure of the porous Al_2O_3 matrix and to the magnetic properties of the nanowire system. As was shown in Refs. [5,6], the small angle diffraction on these objects should be described by the scattering theory beyond the Born approximation. Among the advantages of the method is the fact that information about structure is obtained over the whole volume of the sample [7]. It is worthwhile to note that the picture of the scattering from the ordered system of the magnetic nanowires is not trivial because the complicated system of the demagnetizing fields appeared in the sample upon magnetization process [8,9].

Preparation of spatially ordered arrays of cobalt nanowires was carried out by metal electrocrystallization inside the channels of

---

[*] Corresponding author.
E-mail address: chumakov@lns.pnpi.spb.ru (A.P. Chumakov).

0921-4526/$ - see front matter © 2010 Elsevier B.V. All rights reserved.
doi:10.1016/j.physb.2010.10.081

anodic alumina films with a thickness of 110 μm. In order to obtain better ordering of the channels, the anodic aluminium oxide membranes were prepared by the two-step anodization technique [10,11]. The anode oxidation of aluminium is performed in a two-electrode electrochemical cell in a 0.3 M $(COOH)_2$ solution at a DC voltage of 40 V for 50 and 42.5 h in the first and second anodization stages, respectively. The procedure of fabrication of electrodes on AAO films is described in details elsewhere [8,12].

Electrodeposition of cobalt was carried out in three-electrode cell from 0.3 M $CoSO_4$+0.05 M $CoCl_2$+0.3M H_3BO_3 solution at deposition potential $E_d = -0.8$ V versus Ag/AgCl reference electrode using Autolab PGSTAT 302 potentiostat. The Pt wire serves as a counter electrode. The duration of the Co electrodeposition was 3 h, which corresponds, according to scanning electron microscopy, to the formation of nanowires with a length of 100 μm and a diameter of about 40 nm. Fig. 1 presents the SEM pictures of a side view of the AAO film with arrayed Co nanowires on a bottom part.

Polarized SANS measurements were carried out at the SANS-2 beamline of Geesthacht Neutron Facility (GeNF). Polarized neutron beam with mean wavelength of $\lambda = 0.5$ nm, wavelength spread of $\Delta\lambda/\lambda = 10\%$, and initial polarization $P_0 = 0.95$ was used. A film with an area of 0.3 cm^2 was oriented perpendicularly to the neutron beam and was uniformly irradiated over the entire area. Such an orientation of the sample corresponds to parallel orientation of the pores and the long axis of the magnetic nanowires to the incident neutron beam. The chosen geometry of the experiment allows the observation of diffraction reflections from the ordered system of pores or magnetic wires in a small-angle scattering range. The sample-to-detector distance of 14 m was used with appropriate collimations to cover scattering vectors Q from 0.03 to 0.18 nm^{-1}. An external magnetic field (up to 800 mT) was applied in the horizontal plane perpendicular to the incident beam (and perpendicular to the long axis of the nanowires). The SANS data were taken at 0 mT before the remagnetization experiment. It had been subtracted from SANS data taken under applied magnetic field. The data were given at temperature 290 K. We determine the total (nuclear and magnetic) scattering $(I(Q) = I^+(Q) + I^-(Q))$ and the polarization dependent part of the scattering $(\Delta I(Q) = I^+(Q) - I^-(Q))$, where $I^+(Q)$ and $I^-(Q)$ are the intensities for neutrons polarized parallel (+) and anti-parallel (–) to the magnetic field. The field-dependent scattering intensity is extracted as $I_H(Q) = I(Q,H) - I(Q,0)$. Data were taken at temperature 290 K. The alpha-dependence is not statistically resolved for our measurements since the obtained magnetic signal is rather weak. We are forced to average the intensity over an azimuth angle in order to reach a reasonable signal-to-noise ratio.

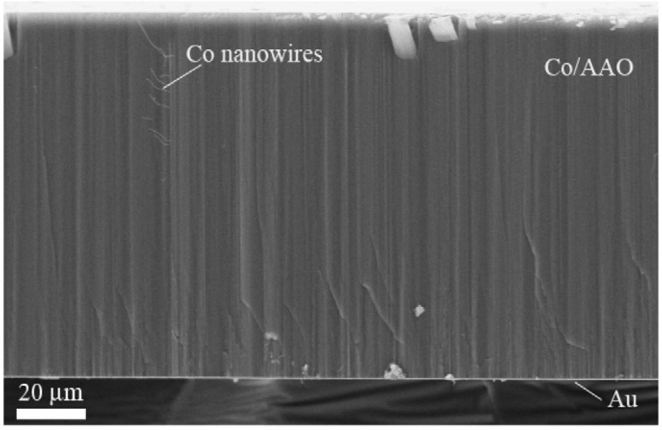

Fig. 1. The SEM data: a side view of the anodic alumina film with arrayed Co nanowires.

A magnetization curve with applied magnetic field in the plane of the film (perpendicular to the nanowires axis) were recorded using SQUID magnetometer Cryogenics S-700 at temperature 290 K. Fig. 2 presents the magnetization curve, saturated at $\mu_0 H = 700$ mT. A small hysteresis loop is observed in the range from -300 to 300 mT. Such form of remagnetization curve with the hysteresis loop is typical for long nanowires at the magnetic field, applied perpendicularly to their axis [1]. We believe that in our case the *c*-axis of Co crystallites is randomly oriented. The loop in Fig. 2 is not rectangular, similar to Ni nanowires, where the shape anisotropy dominates and one cannot distinguish whether shape or magnetocrystalline anisotropy is predominant. Furthermore we can conclude that according to the SANS data in our cobalt array, a magnetocrystalline anisotropy plays the major role.

A typical neutron diffraction pattern measured from Co nanowire array grown inside AAO membrane is shown in Fig. 3a. The first and the second order reflections have been detected, suggesting the presence of strong correlations in the positions of the pores (or nanowires) over significant distances. The hexagonally arranged set of reflections demonstrates the 6-fold symmetry of the structure.

The widening of reflections to 10–20° in an azimuthal direction, shown in Fig. 3a, indicates that samples have a block structure, with slight disorientation of domains in the plane of the film. Nevertheless, the diffraction patterns, typical for a quasi-single crystal, were recorded using a neutron beam of 5 mm diameter, suggesting correlated orientation of the domains on the irradiated area ($\sim$0.3 cm^2). Similar results had been observed previously for pure anodic aluminium oxide membranes by SANS techniques [5,6].

Fig. 3b illustrates the momentum-transfer dependence of the total (nuclear and magnetic) neutron scattering $I(Q)$ for the nonmagnetized ($\mu_0 H = 1$ mT) and magnetized ($\mu_0 H = 800$ mT) sample. Several diffraction maxima are clearly observed, indicating the highly ordered structure of the Co/Al_2O_3 nanocomposite. The momentum transfer dependence $I(Q)$ is satisfactorily reproduced by the sum of the Gaussian components with the centers located at $Q_{10} = 0.069 \pm 0.004$ nm^{-1}, $Q_{11} = 0.119 \pm 0.004$ nm^{-1}, $Q_{20} = 0.138 \pm 0.004$ nm^{-1}, and fixed half-width of $w = 0.0090 \pm 0.0005$ nm^{-1}; coupled with a diffuse small-angle scattering, represented by an exponential decay. The observed diffraction maxima are classified in the hexagonal lattice with the parameter $a = 106 \pm 2$ nm. It should be noted that applying the external magnetic field induces noticeable increase in the diffraction peak intensity in the order of 6% (see Fig. 3b).

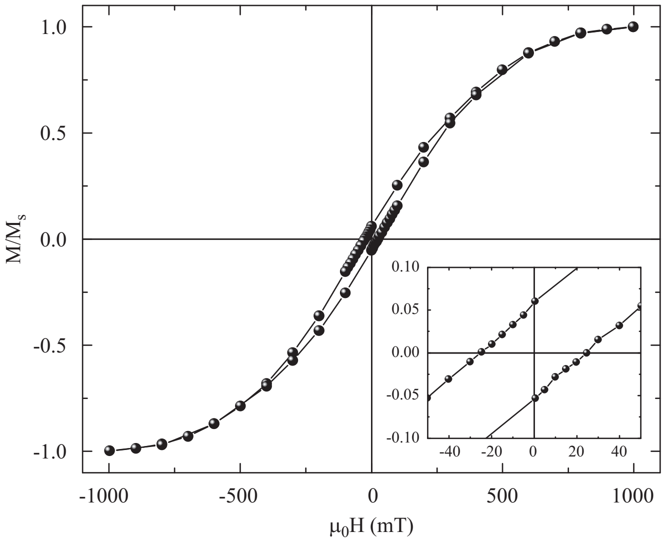

Fig. 2. Magnetization curve for Co nanowires embedded into alumina membrane in the field applied perpendicular to the long axis of the wires.

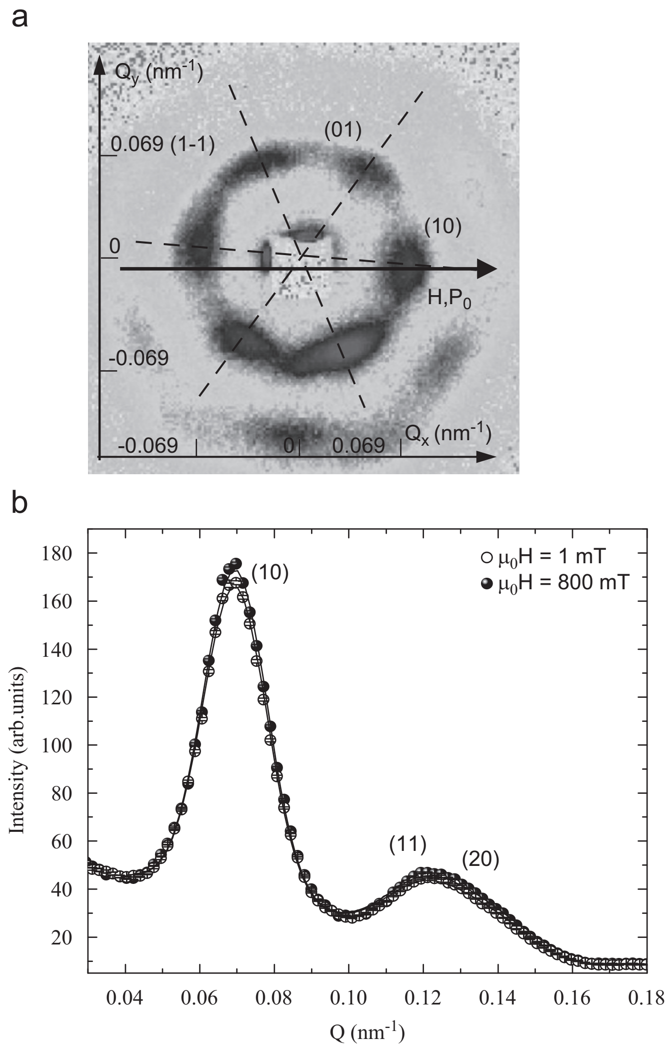

Fig. 3. Typical 2D neutron diffraction pattern from Co/Al$_2$O$_3$ nanocomposite with spatially ordered structure (a). Momentum-transfer dependence of the total (nuclear and magnetic) neutron scattering intensity at $\mu_0H=1$ and 800 mT (b).

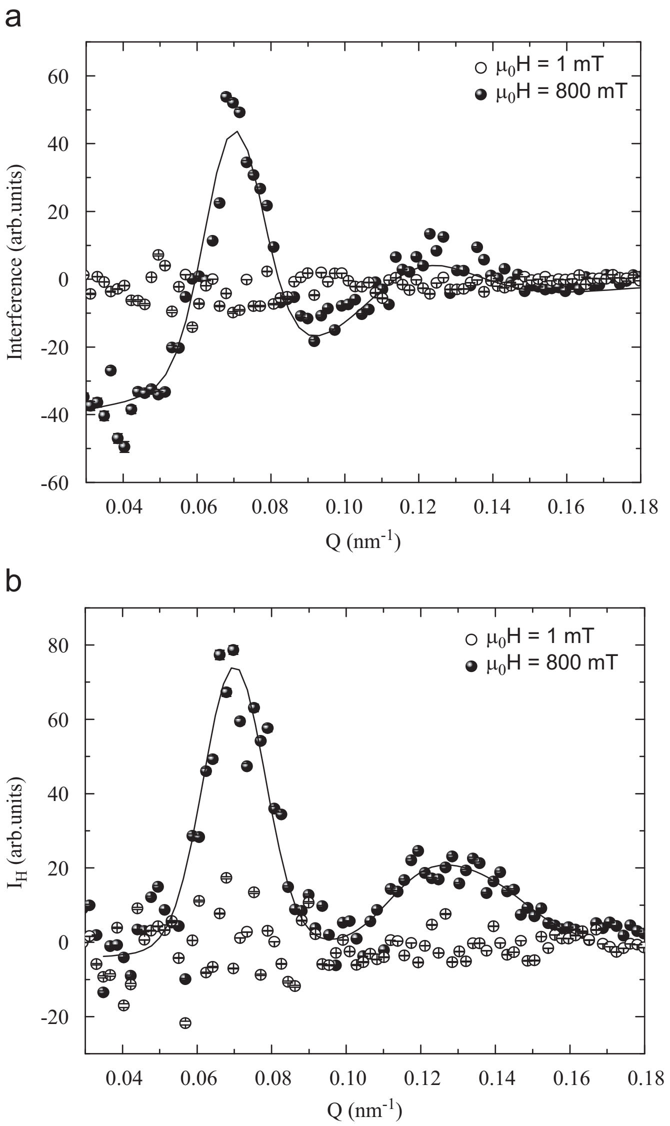

Fig. 4. Q-dependence of the nuclear–magnetic interference $\Delta I(Q)$ at $\mu_0H=1$ and 800 mT (a) and magnetic contribution to the scattering $I_H(Q)$ (b).

Fig. 4 shows the nuclear–magnetic interference $\Delta I(Q)$ and the field-dependent part of neutron scattering $I_H(Q)$ as a function of scattering vector. The peak positions for the magnetic contributions match the positions of nuclear peaks (at zero magnetic field in Fig. 3b). This confirms the formation of the spatially ordered magnetic structure, e.g. the ordered array of nanowires with periodicity of 106 nm.

As seen from Fig. 4a, the interference contribution $\Delta I(Q)$ is equal to zero in the entire momentum-transfer range for the unmagnetized sample ($\mu_0H=1$ mT). In high magnetic fields, the polarization-dependent scattering consists of two contributions: interference maxima at Q values coinciding with the positions of diffraction reflections in scattering on the ordered structure of nanowires and interference in diffuse small-angle scattering. These two contributions have opposite signs in a good agreement with theory [8]. The interference scattering can be approximated by the sum of the Gaussians with the centers at zero (diffuse scattering) and at $Q=Q_{hk}$ (coherent scattering). The magnetic field dependence of the interference contribution integrated over the azimuthal angle at $|Q_{10}|$ and diffusion scattering are shown in Fig. 5a. Note that the interference contribution is proportional to the average magnetization, which exhibits no hysteresis within error bars in initial magnetization or in subsequent remagnetization of the system of magnetic nanowires in the field perpendicular to the long axis of wires. It is interesting to note that an increase in intensity is gradual and has a tendency to the saturation with increase in the magnetic field above 600 mT. This behavior coincides with the data of magnetization curve obtained from SQUID, Fig. 2.

The magnetic-field-dependent scattering component $I_H(Q)$ shown in Fig. 4b represents the difference between the magnetic cross-sections of the sample in two significantly different states, a state close to saturation magnetization (in a field of $\mu_0H=800$ mT) and a completely demagnetized state. The main component of the magnetic cross-section at $\mu_0H=800$ mT is the system of the magnetic reflections described by the sum of Gaussians whose positions correspond to the maxima of the nuclear scattering cross-section. On the contrary, the main component of the cross-section in zero magnetic field is scattering on domains, i.e., diffuse scattering, which is described by a Gaussian at $Q=0$ with no contribution to diffraction reflections. The magnetic field dependence of the integral intensity of magnetic reflection at $Q=|Q_{10}|$ is shown in Fig. 5b. The intensity does not change within error bars in the range from 0 up to 200 mT. Then the negligible increase occurs up to a point of the saturation field. Thereafter, upon decreasing field the magnetic intensity component rises up rapidly with subsequent smooth decrease to the field value of 200 mT. A similar

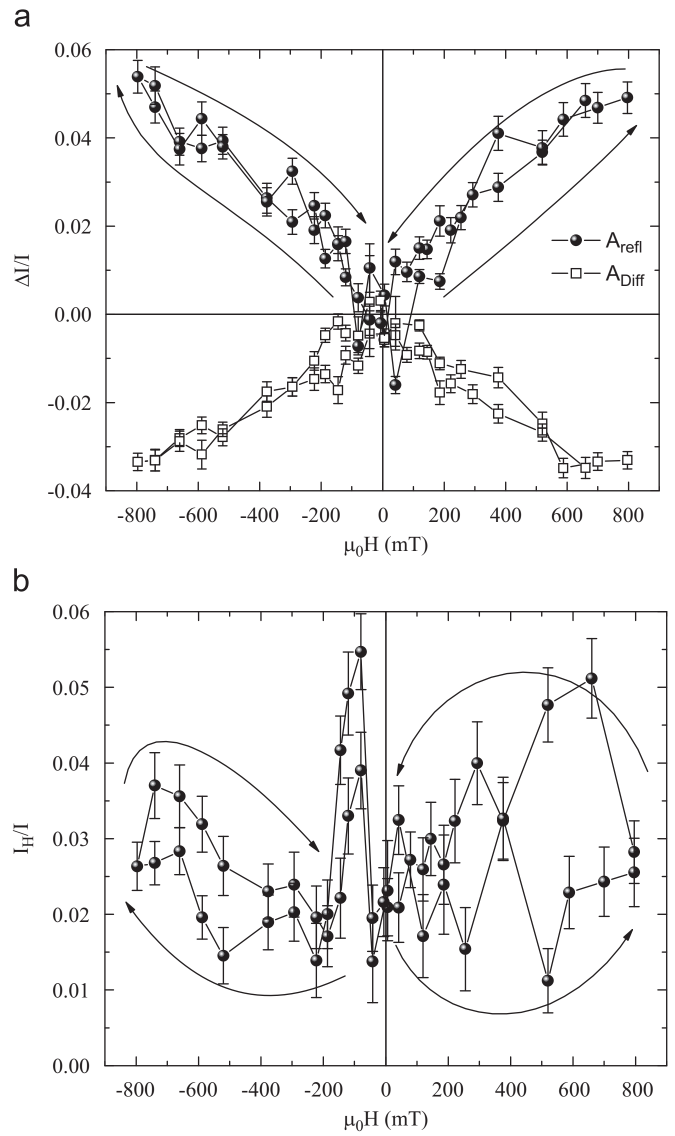

Fig. 5. Magnetic field dependence (a) of the interference contributions (diffusive and coherent) and (b) the magnetic coherent contribution obtained from the approximation of the experimental data.

behavior occurred at the reverse magnetization process. It is worth noting that such a "butterfly" curve of magnetic contribution in dependence of the magnetic field are observed in the other magnetic arrays structures [8,13]. The "butterfly" curve is usually observed from different types of magnetic nanowires arrays in polarized SANS experiment, when the field is perpendicular to the wire axis. In our case the "butterfly" curve is hardly statistically resolved; however, it can be seen that subsequent increase and decrease in the magnetic field produce two curves: the first one lays lower than the second one. Some instability of the magnetic sample under investigation is observed at $\mu_0 H = -100$ mT. The nature of this instability remains unknown.

It should be noticed that value of magnetic contribution reaches 6% from the total intensity only. This contradicts obviously to the fact that the nuclear scattering amplitude of cobalt (0.28–10^{-12} cm) is twice as smaller as the magnetic scattering amplitude (0.47–10^{-12} cm) [14]. One would expect that the magnetic scattering from Co nanowires should be 4 times larger than the nuclear one. This disagreement between the expected and the measured values for magnetic contribution can be explained if one takes into account that the coherent volume for the nuclear scattering is much larger than the coherent volume for the magnetic scattering [5]. Consequently, nuclear part has become predominant over magnetic one.

To explain the small values for the coherent volume of the magnetic scattering, we suppose that the cobalt nanowires consist of small single crystal parts, forming a polycrystalline wire. The magnetic moments in two neighboring crystallites pointing along the *c*-axis of the HCP crystallographic structure are most probably directed differently. The applied magnetic field ($\mu_0 H > 1$ T) cannot turn the magnetization toward the field axis thus producing out of single wire a very inhomogeneous magnetic object with low coherent volume. Thus one can conclude that it is crystallographic anisotropy of Co crystallites of the wire but not the wire's shape anisotropy that plays the crucial role in the magnetization process of the massive of Co nanowires.

In conclusion, we have investigated the process of the remagnetization of the Co nanowires arrays in the magnetic field applied perpendicularly to the long wire's axis. It has been illustrated that polarized neutron scattering provides unique information inaccessible by the standard magnetometry techniques, namely, an anomalously low value of the magnetic contribution as compared with nuclear one. This behavior is interpreted in terms of low coherent volume magnetic structure as compared with the relatively large coherent volume of the nuclear one.

The Russian authors are grateful to the GKSS Research Centre (Germany) for hospitality and also thank RFBR for the support (Grant nos. 10-02-00634).

References

[1] S. Goolaup, N. Singh, A.O. Adeyeye, V. Ng, M.B.A. Jalil, Eur. Phys. J. B. 44 (2005) 259.
[2] E.C. Stoner, E.P. Wohlfarth, Philos. Trans. R. Soc. 240 (1948) 599.
[3] W.F. Brown, Phys. Rev. 105 (1957) 1479.
[4] M. Jaafar, R. Yanes, D. Perez de Lara, O. Chubykalo-Fesenko, A. Asenjo, E.M. Gonzalez, J.V. Anguita, Phys. Rev. B. 81 (2010) 054439.
[5] S.V. Grigoriev, A.V. Syromyatnikov, A.P. Chumakov, N.A. Grigoryeva, K.S. Napolskii, I.V. Roslyakov, A.A. Eliseev, A.V. Petukhov, H. Eckerlebe, Phys. Rev. B. 81 (2010) 125405.
[6] S.V. Grigoriev, N.A. Grigorieva, A.V. Syromyatnikov, K.S. Napolskii, A.A. Eliseev, A.V. Lukashin, Yu.D. Tretyakov, H. Eckerlebe, JETP Lett. 85 (2007) 449.
[7] K.S. Napolskii, I.V. Roslyakov, A.A. Eliseev, A.V. Petukhov, D.V. Byelov, N.A. Grigoryeva, W.G. Bouwman, A.V. Lukashin, K.O. Kvashnina, A.P. Chumakov, S.V. Grigoriev, J. Appl. Cryst. 43 (2010) 531.
[8] S.V. Grigoriev, N.A. Grigorieva, A.V. Syromyatnikov, K.S. Napolskii, A.A. Eliseev, A.V. Lukashin, Yu.D. Tretyakov, H. Eckerlebe, JETP Lett. 85 (2007) 605.
[9] S.V. Grigoriev, A.P. Chumakov, A.V. Syromyatnikov, N.A. Grigorieva, A.I. Okorokov, K.S. Napol'skii, I.V. Roslyakov, A.A. Eliseev, A.V. Lukashin, H. Eckerlebe, Solid State Phys. 52 (2010) 1080.
[10] H. Masuda, K. Fukuda, Science 268 (1995) 1466.
[11] S. Shingubara, J. Nanoparticle Res. 5 (2003) 17.
[12] G. Sauer, G. Brehm, S. Schneider, K. Nielsch, R.B. Wehrspohn, J. Choi, H. Hofmeister, U. Gosele, J. Appl. Phys. 91 (2002) 3243.
[13] N.A. Grigoryeva, S.V. Grigoriev, H. Eckerlebe, A.A. Eliseev, A.V. Lukashin, K.S. Napolskii, J. Appl. Cryst. 40 (2007) s532.
[14] G.E. Bacon, K. Lonsdale, Rep. Prog. Phys. 16 (1953) 1.